



Multizone Decomposition for Simulation of Time-Dependent Problems Using the Multiquadric Scheme

A. S. M. WONG

Department of Mathematics, City University of Hong Kong
Hong Kong
and

Open University of Hong Kong, 30 Good Shepherd Street
Homantin, Kowloon, Hong Kong

Y. C. HON

Department of Mathematics, City University of Hong Kong
Hong Kong

T. S. LI AND S. L. CHUNG

Open University of Hong Kong, 30 Good Shepherd Street
Homantin, Kowloon, Hong Kong

E. J. KANSA

Lawrence Livermore National Laboratory
Livermore, CA 94551, U.S.A.

(Received April 1998; revised and accepted November 1998)

Abstract—This paper discusses the application of the multizone decomposition technique with multiquadric scheme for the numerical solutions of a time-dependent problem. The construction of the multizone algorithm is based on a domain decomposition technique to subdivide the global region into a number of finite subdomains. The reduction of ill-conditioning and the improvement of the computational efficiency can be achieved with a smaller resulting matrix on each subdomain. The proposed scheme is applied to a hypothetical linear two-dimensional hydrodynamic model as well as a real-life nonlinear two-dimensional hydrodynamic model in the Tolo Harbour of Hong Kong to simulate the water flow circulation patterns. To illustrate the computational efficiency and accuracy of the technique, the numerical results are compared with those solutions obtained from the same problem using a single domain multiquadric scheme. The computational efficiency of the multizone technique is improved substantially with faster convergence without significant degradation in accuracy. © 1999 Elsevier Science Ltd. All rights reserved.

Keywords—Multizone, Decomposition, Hydrodynamics equation, Multiquadric.

1. INTRODUCTION

In this paper, we set up an efficient algorithm applicable to the Multiquadric method (MQ) for solving large scale time-dependent problems. This scheme uses a similar computational procedure

This research is supported by the Research and Development Fund of the Open University of Hong Kong, # 1.7/96 and the Research Grant Committee of City University of HK, #9040286.

The authors wish to thank the Royal Observatory of Hong Kong for providing meteorological data for numerical computation.

in each zone that can be readily parallelized. The efficiency of the computation is improved significantly without sacrificing accuracy since the size of each resulting coefficient matrix is much smaller. The multiquadric method is employed for the spatial approximation together with an explicit forward finite difference scheme for the time-dependent integration.

The multiquadric method was developed by Hardy [1] in 1970 to interpolate two-dimensional geographical surfaces. Hardy's multiquadric basis function had been reviewed and modified by Kansa [2,3] and Hon *et al.* [4,5] for solving physical equations with ordinary and partial differential equations. A number of experiments of the method had been carried out and tested by Kansa and other researchers in various scientific and engineering disciplines. The application results were found to be significantly better with other well-established methods, such as finite difference and finite element schemes. It has been successfully applied to our previous study of a water quality model [6].

The ease of implementation and good computational performance of the method make it a very attractive alternative to other traditional methods. In addition, the method has the advantage of mesh free implementation. The high flexibility of the method makes it very suitable for domains with highly irregular boundaries. However, the multiquadric method has a drawback which is the requirement of the solution of a full global coefficient matrix which could be computationally intensive and may cause instability if the matrix is ill-conditioned. Computational efficiency is a major factor to be considered in solving large-scale problems with large number of collocation points.

The multizone decomposition scheme is a combination of the domain decomposition and the MQ method. In this scheme, the region under study is divided into a number of nonoverlapping finite zones. The number of interpolation points in each zone is a subset of the entire domain. To maintain the continuity across the zones, points adjacent to the zone boundaries, as well as an additional set of sparse data points from other zones and from the natural boundaries are included to form a set of computational data points, where MQ computation of each zone is applied to this set of data in a similar manner as the global MQ simulation. The resulting matrix for the computation of each set of data points is much smaller than that using a single global multiquadric matrix. Justification for not using iterative corrections to remedy smoothness across boundaries will be described in Section 4.

Section 2 discusses the basic theory of the underlying hydrodynamic equations. Section 3 introduces the application of the multiquadric method. The concept of the multizone decomposition technique applied to the multiquadric interpolation scheme as well as the computational complexity analysis are described in Section 4. Numerical results are presented in Section 5. Finally, the paper ends with a conclusion in Section 6.

2. GOVERNING EQUATIONS

In this paper, we introduce a multizone decomposition algorithm to solve a set of time-dependent nonlinear partial differential equations using the multiquadric method. For the sake of comparison, we employ the same set of hydrodynamic equations which was used in a water quality model in a previous study [6]. The governing equations are the two-dimensional depth-integrated version of three differential equations, namely the continuity equation and the momentum conservation equations in the x and y directions, respectively, in a region Ω . These equations are expressed in vector notation as

$$\frac{\partial \Phi}{\partial t} + \frac{\partial \mathbf{G}}{\partial x} + \frac{\partial \mathbf{F}}{\partial y} + \mathbf{E} = 0, \quad \text{in } \Omega \subset R^2, \quad (2.1)$$

where Φ , \mathbf{G} , \mathbf{F} , \mathbf{E} are column vectors given as

$$\Phi = \begin{pmatrix} \zeta \\ u \\ v \end{pmatrix}, \quad \mathbf{G} = \begin{pmatrix} uH \\ u^2 \\ uv \end{pmatrix}, \quad \mathbf{F} = \begin{pmatrix} vH \\ uv \\ v^2 \end{pmatrix},$$

$$\mathbf{E} = \begin{pmatrix} 0 \\ g \left(\frac{\partial \zeta}{\partial x} + \frac{u\sqrt{u^2 + v^2}}{HC_b^2} \right) - fv - \frac{\rho_a}{H\rho_w} C_s W_x W_s \\ g \left(\frac{\partial \zeta}{\partial y} + \frac{v\sqrt{u^2 + v^2}}{HC_b^2} \right) + fu - \frac{\rho_a}{H\rho_w} C_s W_y W_s \end{pmatrix},$$

where u, v are the depth-averaged advective velocities in x, y directions, respectively; ζ is the sea water surface elevation; h is the mean depth of sea level; H is the total depth of sea level, such that $H = h + \zeta$; W_x, W_y are the wind velocity components in x, y directions, respectively, and W_s is the wind speed given as $W_s = \sqrt{W_x^2 + W_y^2}$. C_b is the Chezy bed roughness coefficient; f is the coriolis force parameter; g is the gravitational acceleration; ρ_a is the density of air; ρ_w is density of water, and C_s is the surface friction coefficient. The water-water boundary condition is defined as

$$\zeta(x, y, t) = \zeta^*(x, y, t), \quad (2.2)$$

where $\zeta^*(x, y, t)$ is the specific sea surface elevation level on the water-water boundary. The water-land boundary condition is defined as

$$\mathbf{Q} \cdot \mathbf{N} = 0, \quad (2.3)$$

where \mathbf{Q} represents the velocity vector (u, v) , \mathbf{N} is the direction of the outward normal vector on the land boundary. At the n^{th} time step, the current velocities (u^n, v^n) on the land boundary are derived from this condition as

$$\begin{aligned} u^n(x_i, y_i) &= \tilde{u}^n(x_i, y_i) \sin^2(\theta_i) - \tilde{v}^n(x_i, y_i) \sin(\theta_i) \cos(\theta_i), \\ v^n(x_i, y_i) &= \tilde{v}^n(x_i, y_i) \cos^2(\theta_i) - \tilde{u}^n(x_i, y_i) \sin(\theta_i) \cos(\theta_i), \end{aligned} \quad (2.4)$$

where $\tilde{u}^n(x_i, y_i)$ and $\tilde{v}^n(x_i, y_i)$ are the values computed at data point (x_i, y_i) on the land boundary from the multiquadric interpolant, θ_i is the outward normal angles at the water-land boundary points which are computed by taking the average of the vectors joining the neighbouring points. The initial conditions are

$$\begin{aligned} \mathbf{Q}(x_i, y_i, 0) &= \mathbf{0}, \\ \zeta(x_i, y_i, 0) &= 0, \end{aligned} \quad (2.5)$$

for all $x_i, y_i \in \Omega$. We solve the numerical time discretization for equation (2.1) using a forward finite difference method and the corresponding partial derivatives by multiquadric scheme. The numerical solution on the boundaries are updated at each time step by the corresponding conditions. The surfaces elevation ζ^n on the open sea boundary is specified by the boundary condition given in equation (2.2). Similarly, we updated the flow velocities u^n, v^n on the land boundaries at each time step using equation (2.4).

In this report, a simple Euler forward difference time discretization scheme is chosen to solve the time-dependent problem. The main purpose of the project is to investigate the applicability and efficiency of the multizone MQ scheme in comparison with the global MQ scheme. Hence, for the sake of comparison, a simple time discretization scheme is chosen to avoid any complexity arising if a more sophisticated time discretization scheme is chosen. Furthermore, owing to the requirement of updating information on both land and water boundaries in each time step to fulfill the open sea and land boundaries conditions, the use of large time-step may not be a adequate choice to do the computation. This is because the error propagation and smoothing effect could be increased due to the rare information input from the open sea boundary.

To maintain the stability, the time-step size is restricted by the Courant number which is chosen to satisfy the following condition:

$$\Delta t \leq \frac{d_{\min}}{\sqrt{gh}}, \quad (2.6)$$

where d_{\min} is the minimum distance between any two adjacent collocation points and h is the average water depth between the two points. This condition will ensure that the time truncation errors in the interior will not be propagated.

3. APPLICATION OF MULTIQUADRIC METHOD

The basic concept of the multiquadric method is to interpolate an unknown function $M(P)$ using a finite series of radial basis functions at N given distinct points P_j . The MQ radial functions are written as

$$M(P) \simeq \sum_{j=1}^N \alpha_j (\|P - P_j\| + r^2)^{1/2}, \quad (3.7)$$

where $P_j \in \mathbf{R}^2$, $j = 1, 2, \dots, N$ and α_j s are the unknown coefficients to be calculated. $\|P - P_j\|$ is the Euclidean distance. The shape of the basis functions is entirely controlled by varying the magnitude of the shape parameter $r > 0$. When r is small, the basis function fits a spiky surface to the data points. As r increases, the spikes at the data points spread out to form a smooth surface. When r is too large and reaches a critical value, the resultant matrix becomes extremely ill-conditioned and the numerical error increases dramatically. In [7], the authors used a constant value of r and found a heuristic recipe for its value for different functions. Kansa *et al.* have reported their investigation on the effect of the shape parameter as regards to multiquadric interpolation function in [2,8]. They found that the computational accuracy of the interpolant can be improved by varying the shape parameter with the basis function. They employed numerical experiments to resolve the optimal shape factor r^2 given by

$$r_i^2 = r_{\min}^2 \left(\frac{r_{\max}^2}{r_{\min}^2} \right)^{(i-1/N-1)}, \quad (3.8)$$

r_{\min}^2 and r_{\max}^2 are preset parameters. Lately Golberg *et al.* [9] used statistical method of cross validation to determine the optimal shape parameter and the method has been successfully implemented with satisfactory results.

Currently some theoretical studies on the choice of the optimal shape parameter are still in progress by other researchers. The lack of the mathematical theory makes it very difficult to choose a suitable r^2 for the current study. For the sake of simplicity, we adopt the suggested value from the original Hardy's scheme [1] by letting r be $0.815 d_{\min}$, where d_{\min} is the minimum distance between any two interpolation points in the study region. The sensitivity of the numerical results to the shape parameter have been examined with a linear hydrodynamic equation. The results are computed for a range of shape parameter starting from $r = 0.1 d_{\min}$ until the solution diverges. The analysis shows that a near-optimal approximation of the model can be achieved by using the proposed value $0.815 d_{\min}$.

To solve the time-dependent differential equations, the governing equation (2.1) are integrated in time using explicit forward difference scheme given as

$$\Phi_i^{n+1} = \Phi_i^n - \Delta t \left(\frac{\partial \mathbf{G}_i^n}{\partial x} + \frac{\partial \mathbf{F}_i^n}{\partial y} + \mathbf{E}_i^n \right) \quad (3.9)$$

where Δt is the time step, Φ_i^{n+1} is the solution vector at the points (x_i, y_i) in time $n\Delta t$. The numerical values for the corresponding spatial derivatives are obtained by the multiquadric interpolation scheme.

The values of the multiquadric interpolant Φ^n are given by the following radial basis function:

$$\Phi^n(x, y) = \sum_{j=1}^N \alpha_j^n \left[(x - x_j)^2 + (y - y_j)^2 + r^2 \right]^{1/2}. \quad (3.10)$$

The unknown coefficients vector $[\alpha_j^n]$ are determined by collocating with a set of data points $(x_i, y_i)_{i=1}^N$ over the domain Ω given as

$$\Phi^n(x_i, y_i) = \sum_{j=1}^N \alpha_j^n \left[(x_i - x_j)^2 + (y_i - y_j)^2 + r^2 \right]^{1/2}, \quad (3.11)$$

which forms a system of N linear equations in N unknowns

$$\begin{pmatrix} \Phi_1^n \\ \Phi_2^n \\ \vdots \\ \Phi_N^n \end{pmatrix} = \begin{pmatrix} q_1(x_1, y_1) & q_2(x_1, y_1) & \cdots & q_N(x_1, y_1) \\ q_1(x_2, y_2) & q_2(x_2, y_2) & \cdots & q_N(x_2, y_2) \\ \vdots & \vdots & \ddots & \vdots \\ q_1(x_N, y_N) & q_2(x_N, y_N) & \cdots & q_N(x_N, y_N) \end{pmatrix} \begin{pmatrix} \alpha_1^n \\ \alpha_2^n \\ \vdots \\ \alpha_N^n \end{pmatrix}, \quad (3.12)$$

where

$$q_j(x_i, y_i) = \sqrt{(x_i - x_j)^2 + (y_i - y_j)^2 + r^2}.$$

For simplicity, we express the system of equation by matrix form

$$A\vec{\alpha} = \vec{\Phi}, \quad (3.13)$$

where $A = [q_j(x_i, y_i)]$ is an $N \times N$ coefficient matrix; $\vec{\alpha} = [\alpha_j^n]$ and $\vec{\Phi} = [\Phi_j^n]$ are $N \times 1$ matrices. The unknown coefficients vector $[\alpha_j^n]$ can be determined using Gaussian elimination. Micchelli [10] has shown that multiquadric interpolation function is a type of conditionally positive definite functions, and therefore, the coefficient matrix for the N linear equations in (3.12) is invertible for distinct points (x_i, y_i) . Powell [11] has shown that the guaranteed invertibility of the coefficient matrix for all radial basic functions can be achieved by adding a polynomial term into equation (3.7). Carlson [7] reviewed that adding the polynomial term to the MQ interpolant is not an improvement. It is advisable to add a constant term to maintain the stability instead of polynomial term. However, Powell [11] further proved that the interpolation matrix of the multiquadric radial function as given in equation (3.7) is nonsingular for any set of distinct interpolation points, and that the invertibility is guaranteed. Therefore, adding the constant term to the MQ interpolant is not generally required.

The MQ expansion equations (3.10) and (3.11) are positive definite. The partial derivative terms of these two equations are also conditionally positive definite as all the MQ basis functions are continuously differentiable. If the PDE problem is properly posed, then the PDE coefficient matrix which is constructed from a linear combination of functions and partial derivatives will also be positive definite, hence invertible. Improperly posed PDE problems may not be invertible. Furthermore, to ensure the PDE problem is to be invertible, the following conditions must be met:

- (1) all points belonging to the interior and boundary problem must be distinct,
- (2) the interior points must be distinct from the locus of the boundaries, and
- (3) a finite shape parameter distribution must be used.

The first partial derivatives of the vector function $\Phi_i^n(x_i, y_i)$ with respect to x and y are given, respectively, as follows:

$$\frac{\partial \Phi^n(x_i, y_i)}{\partial x} = \sum_{j=1}^N \alpha_j^n (x_i - x_j) q_j^{-1}(x_i, y_i); \quad (3.14)$$

$$\frac{\partial \Phi^n(x_i, y_i)}{\partial y} = \sum_{j=1}^N \alpha_j^n (y_i - y_j) q_j^{-1}(x_i, y_i). \quad (3.15)$$

The solution of the interior data points is solved by substituting (3.11) and the partial derivatives (3.14) and (3.15) into equation (3.9) with the given boundary conditions.

The MQ scheme has been successfully applied to many linear and nonlinear equations. We employed the scheme to solve a system of nonlinear water quality model in our previous study [6] and a good agreement with the observed results is indicated. In this study, a new multizone decomposition algorithm is developed to improve the computational efficiency of the MQ scheme. The use of multizone decomposition algorithm is to be introduced in the next section.

4. MULTIZONE DECOMPOSITION FOR MULTIQUADRIC SCHEME

A general discussion and the theory of the use of domain decomposition with multiquadric scheme were presented in [12] by Kansa. He remarked that the method has been proven to be very computationally efficiency and the accuracy have been considerably improved. He also advocated in [8] that two approaches can be considered in solving dense system of linear equations. One approach is to use preconditioning and the other approach is to make use of domain decomposition techniques. Dubal [13] had successfully applied the domain decomposition with blending techniques for multiquadric approximation of second-order partial differential equations in a one-dimensional problem. Dubal concluded that multiquadric interpolation with domain decomposition could accurately solve elliptic PDEs equations and considerably improve the efficiency of computations.

The present study aims to develop a technique to improve the computational efficiency of using multiquadric approximation to solve large-scale time-dependent problems. A multizone decomposition technique is developed together with multiquadric scheme in order to cope with the forementioned computational efficiency problems. Multiquadric method is a grid free scheme which has no restriction on the allocation of data points in any dimensional spaces. The multizone algorithm makes use of this characteristic by incorporating additional set of sparse data points away from each designated zone to enhance the accuracy of the computations in each data point within that zone.

This section describes the detail setup of the multizone decomposition of a two-dimensional problem which is to be solved using the MQ method. Let Ω be the two-dimensional domain under study with a set of data points W defined as

$$W = \{P_j \subset \mathbb{R}^2 \mid j = 1, 2, \dots, N\}. \quad (4.16)$$

Under the multizone decomposition scheme, Ω is divided into K zones Ω^j , $j = 1, 2, \dots, K$, and hence, W is also divided into K subsets of data points W^j , $j = 1, \dots, K$ such that

$$\begin{aligned} W^i \cap W^j &= \emptyset, & \text{if } i \neq j, \\ \bigcup_{i=1}^K W^i &= W. \end{aligned} \quad (4.17)$$

For the zone Ω^k , we denote the set of data points in W^k by

$$W^k = \{P_j^k \mid j = 1, 2, \dots, L_k\}, \quad (4.18)$$

where L_k is the number of data point in subset W^k . In general, there is no criteria in how the subsets of data are to be formed. One possible way is to assign each subset with approximately the same number of data points which leads to load balancing needed for efficient implementation on parallel computers. Parallel computation across zones will be the next phase of our study. For the real-life problem we studied in this project which is the water flow circulation problem in

the Tolo Harbour of Hong Kong, the domain under consideration was divided into several zones according to the geographic and tidal characteristics of the harbour. This way of subdivision will make the results more consistent, since the water flow circulation properties will be quite different under different geographical conditions.

Figure 1 depicts the subdivision of a 2-D domain into three nonoverlapping zones. Computation using the MQ method is applied to the points in each zone Ω^k individually. In order to enhance the accuracy of computation of each zone and to maintain the continuity of the interpolation function across the zone's boundaries, two more sets of extra data points will be added to the set of data points in W^k . The first set includes all the points which are in other zones and adjacent to the boundary of Ω^k denoted as

$$B^k = \{P_j^k \in W^l \mid l \neq k \text{ and } j = L_k + 1, L_k + 2, \dots, L_k + M_k\}, \quad (4.19)$$

where M_k is the total number of data points adjacent to the boundary of Ω^k and is relatively smaller than L_k .

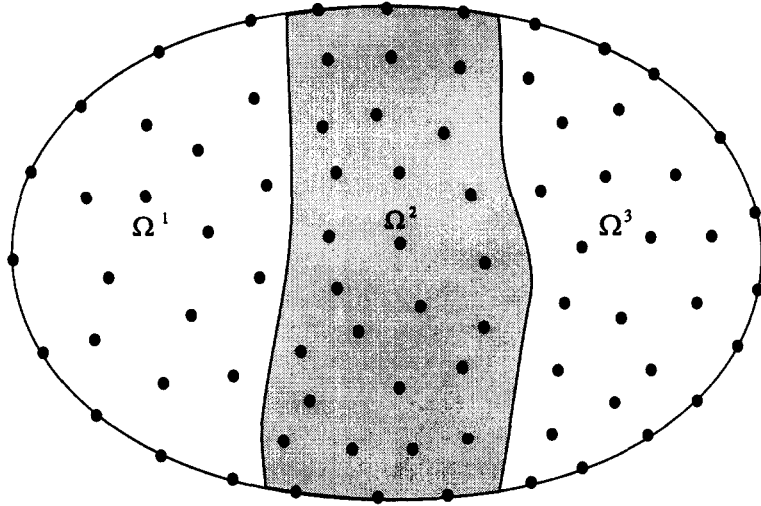


Figure 1. Decomposition of a two-dimensional domain into three zones.

We also include another set of data points which are chosen at random such that they are sparsely and evenly distributed over the other zones in Ω . We denote this set of extra data points as

$$S^k = \{P_j^k \in W^l \mid l \neq k \text{ and } j = L_k + M_k + 1, L_k + M_k + 2, \dots, L_k + M_k + N_k\}, \quad (4.20)$$

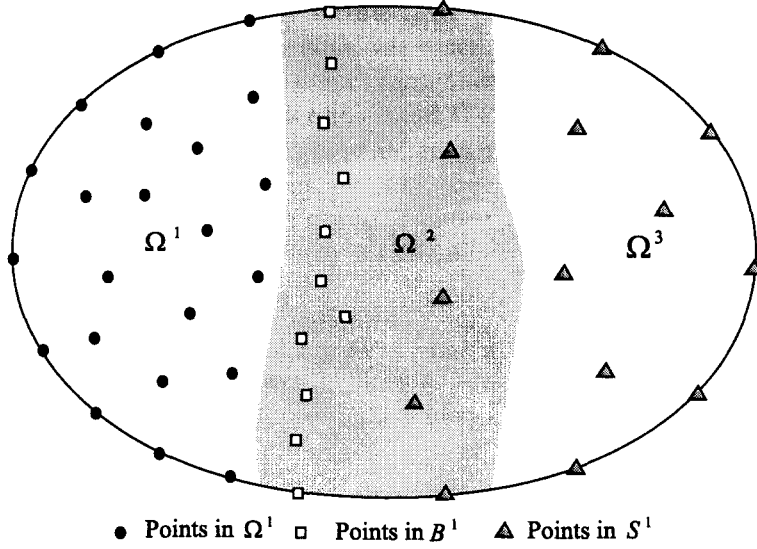
where N_k is also a number of data points relatively smaller than L_k .

Figure 2 depicts the data points to be included when we apply MQ computation to Ω^1 . The points represented by \bullet are data points in W^1 , \square represents data points in B^1 and \triangle represents data points in S^1 . To calculate the solution in each zone Ω^k , MQ computation is applied to the data points in $W^k \cup B^k \cup S^k$ in a similar manner as global MQ simulation. The MQ interpolating function for zone K is given as

$$\Phi_k^n(x_j, y_j) = \sum_{i=1}^{L_k + M_k + N_k} \alpha_i^n \left[(x_j - x_i)^2 + (y_j - y_i)^2 + r_k^2 \right]^{1/2}, \quad (4.21)$$

where n denotes the n^{th} time step and $(x_j, y_j) \in (W^k \cup B^k \cup S^k)$. The shape parameter $r_k = 0.815(d_{\min})_k$ is different in each computational data set, because $(d_{\min})_k$ is determined individually by using the set of collocation points belong to $W^k \cup B^k \cup S^k$.

Distribution of collocating points for computational zone 1



● Points in Ω^1 □ Points in B^1 ▲ Points in S^1
 Figure 2. Distribution of the three different set of collocation points W^1 , B^1 , S^1 in Zone 1.

Having calculated the set of unknown coefficients α_i , for $i = 1, 2, \dots, L_k + M_k + N_k$, the partial derivatives can then be determined for each collocation points $P_j^k \in W^l$, $j = 1, 2, \dots, L_k$, $l = 1, 2, \dots, K$, by the following equations:

$$\frac{\partial \Phi_k^n(x_j, y_j)}{\partial x} = \sum_{i=1}^{L_k + M_k + N_k} \alpha_i^n (x_j - x_i) q_i^{-1}(x_j, y_j); \quad (4.22)$$

$$\frac{\partial \Phi_k^n(x_j, y_j)}{\partial y} = \sum_{i=1}^{L_k + M_k + N_k} \alpha_i^n (y_j - y_i) q_i^{-1}(x_j, y_j). \quad (4.23)$$

These equations only calculate partial derivatives for the collocation points in the subset W^k , since the extra data points in B^k and S^k are from other zones, their partial derivatives are not calculated here. The partial derivative of these points in B^k and S^k would be computed when the zone they belonged to are considered.

It follows that the numerical values $\Phi(x_i, y_i)$ of the next time step $n + 1$ can be calculated using equation (3.9). The values of land and water boundaries are applied similarly as the global MQ computation to update information at each time step using the conditions given in Section 2.

It is noted that the zones only appear when we calculate the partial derivatives $\frac{\partial \Phi_k^n(x_j, y_j)}{\partial x}$ and $\frac{\partial \Phi_k^n(x_j, y_j)}{\partial y}$ using the local interpolation on the data set W^k . When numerical values $\Phi^n(x_i, y_i)$ are calculated using equation (3.9), only local information of the points (x_i, y_i) is required which has all been found in previous time steps. Therefore, no iteration is required in the calculation. The application of the multizone decomposition technique is a simple and effective scheme in comparison with domain decomposition techniques which usually employ iterative methods for boundary and subdomain interface treatment.

To give a better understanding of the computational procedure of the multizone decomposition MQ scheme, the basic algorithm is outlined in Table 1.

Furthermore, it is evident that when the multiquadric method is used to solve initial boundary problems, the result is satisfactory for convex domains. In the MQ method, the shape parameter r controls the fitting of a continuous surface to the data. The shape parameter actually controls the effective number of collocation points used in the interpolation at any location. With proper choice of the shape parameter, interpolation across discontinuities does not usually pose a problem in the application of the MQ method to concave or multiply connected domains. As we

Table 1.

Initialize values $\Phi^0(x_1, y_1), \Phi^0(x_2, y_2), \dots, \Phi^0(x_N, y_N)$; For each step do For each zone $i = 1, 2, \dots, K$ do Calculates unknown coefficients $\alpha_{i,r}$ for points in $(W^i \cup B^i \cup S^i)$ using equation (4.21); For each points in W^i Calculates $\frac{\partial \Phi_k^n(x_j, y_j)}{\partial x}$ and $\frac{\partial \Phi_k^n(x_j, y_j)}{\partial y}$ for points in W^i only using equations (4.22) and (4.23); End for End for For each points $i = 1, 2, \dots, N$ over the global domain Ω do Calculates results $\Phi^n(x_1, y_1), \Phi^n(x_2, y_2), \dots, \Phi^n(x_N, y_N)$ using equation (3.9); for time step $n \rightarrow n + 1$; End for End for.

can see from Figure 5 showing the geographic layout of Tolo Harbour, it contains an irregular coastline and two islands in the outer sea. This forms a concave computational domain. To handle the concavity, a small value of the shape parameter is suggested. The adopted shape parameter $0.815 d_{\min}$ in the present model is sufficient small to assure that the spatial derivatives evaluated at a point are influenced mostly by its immediate neighbouring points and that the interpolation across dry land, which is discontinuous in the computational domain, is minimized in the computational process. Our studies show that the effect of concavity is further improved by using the proposed multizone decomposition MQ method, the subdivision of the domains can handle the concave region better.

4.1. Computational Complexity Analysis

To analyze the computational complexity of the solution of the hydrodynamic equations using the global MQ method, there are several major components of computations we have to consider. First, the unknown coefficients vector $[\bar{\alpha}]$ in equation (3.13) are determined by

$$[\bar{\alpha}] = [\mathbf{A}]^{-1} [\bar{\Phi}], \quad (4.24)$$

where $[\mathbf{A}]$ is the coefficient matrix described in equation (3.12). The inversion of matrix $[\mathbf{A}_{ij}]$ is only required to be calculated once at the beginning of the computation and is used in every time step computation. In equation (4.24), there are N^2 multiplications and $N(N-1)$ additions. Hence, there should be $3(2N^2 - N)$ operations in the calculation of the unknown coefficients vector for the three equations in equation (2.1).

After the computation of the unknown coefficients vector $[\bar{\alpha}]$, the six partial derivative in equations (3.14) and (3.15) can be determined accordingly. In this step, N multiplications and $(N-1)$ additions are needed in obtaining one partial derivative. Since there are N interpolation points over the entire region Ω , therefore $N(2N-1)$ operations are involved for N data points over the region Ω . The calculation of the six partial derivatives should involve in total $6N(2N-1)$ operations.

For the computations of the three interpolants (ζ, u, v) , each of them involves a fixed number of operations, p , where $p \ll N$. Hence, the total number of fixed operations for N data points is $3pN$. Putting all the above operations together, the total number of operations for the major components of computations at a time step is

$$(6N^2 - 3N) + (12N^2 - 6N) + 3pN = 18N^2 + (3p - 9)N. \quad (4.25)$$

For the multizone decomposition MQ scheme, the entire region is first subdivided into k non-overlapped zones with roughly the same number of data points in each zone. We then include a

small portion of approximately rN data points from its neighbouring zones. For each zone, there will be $N/k + rN$ data points involved in the computations. Following the same line of argument, the number of operations required for the computation of a single zone is then given by

$$18 \left(\frac{N}{k} + rN \right)^2 + (3p - 9) \left(\frac{N}{k} + rN \right), \quad k \neq 0. \quad (4.26)$$

To do the computation of the whole region, we need to carry out k sets of computations for the k zones. The total number of operations will be given by

$$k \left[18N^2 \left(\frac{1}{k} + r \right)^2 + (3p - 9)N \left(\frac{1}{k} + r \right) \right], \quad k \neq 0. \quad (4.27)$$

By ignoring the first-order terms in equations (4.25) and (4.27) and comparing the second-order terms, we can see that there will be approximately $[1 - (1/k)(1 + kr)^2]$ percent reduction in operations with the multizone scheme. For the example of our study in Tolo Harbour, we divided the whole study region into $k = 5$ zones with about $r = 14\%$, we will have approximately a 42% saving in computations.

5. MODEL VERIFICATIONS AND NUMERICAL RESULTS

To compare the application of the multizone decomposition MQ scheme with the global multiquadric method, we apply the proposed scheme to a two-dimensional hydrodynamic model. Numerical examples of a linear and a nonlinear model are considered individually to illustrate the efficiency and applicability of the proposed algorithm. The program is written in C++ with double precision on computations and executed on a Pentium PC.

CASE 1. A LINEAR WATER FLOW MODEL. To give a better insight into the multizone MQ algorithm, we firstly apply the method to a linear shallow water equation. This simple model allows a comparison of the computed results with the analytical solution. The equations to be solved are given as

$$\frac{\partial \zeta}{\partial t} + H \nabla \cdot \mathbf{V} = 0, \quad (5.28)$$

$$\frac{\partial \mathbf{V}}{\partial t} = g \nabla \zeta, \quad (5.29)$$

where \mathbf{V} is a vector of the depth-averaged advective velocities in x, y directions, respectively; ζ is the sea water surface elevation; H is the total depth of sea level, such that $H = h + \zeta$; h is the mean depth of sea level; g is the gravitational acceleration. As shown in Figure 3, we generate 205 collocation points in a rectangular channel with length $L = 872$ km, width $W = 50$ km and depth $H = 20$ m, in which 117 collocation points are in the interior, five are on the water-water boundary and 83 are on the land boundary.

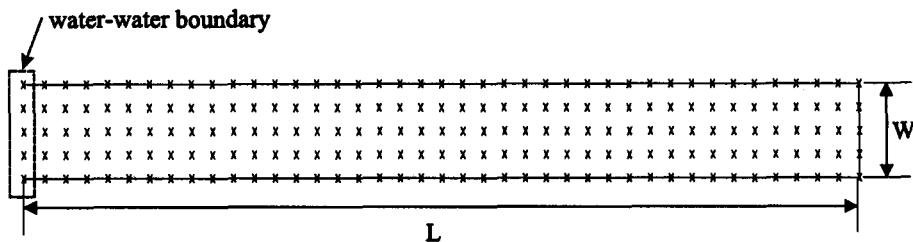


Figure 3. A rectangular channel with 205 collocation points.

On the basis of the multizone MQ algorithm, we first partition the whole region into four nonoverlapped zones, each of these zones contains 51 to 52 collocation points and they are evenly distributed over each zone. For each computational zone, we include another two sets with about 20 extra interpolation points which are placed in its adjacent and neighbouring zones.

The boundary conditions are:

$$\zeta(t)7 = \zeta_0 \cos \omega t, \text{ at } x = 0, \quad 0 \leq y \leq W, \quad (5.30)$$

$$u(t) = 0, \quad \text{at } x = L, \quad 0 \leq y \leq W, \quad (5.31)$$

$$v(t) = 0, \quad \text{at } y = 0, \text{ and } y = W, \quad 0 \leq x \leq W, \quad (5.32)$$

and the initial conditions are:

$$\vec{Q}(x, y, 0) = \mathbf{0}, \quad (5.33)$$

$$\zeta(x, y, 0) = 0, \quad (5.34)$$

where $\zeta_0 = 1 \text{ m}$ and $\omega = 1.45444 \times 10^{-4} / \text{s}$. The analytical solution to this boundary-value problem is known and is given by

$$\zeta(x, y, t) = \zeta_0 \cos \left(\frac{\omega}{\sqrt{gH}} (L - x) \right) \frac{\cos \omega t}{\cos \left(\frac{\omega}{\sqrt{gH}} L \right)}; \quad (5.35)$$

$$u(x, y, t) = -\zeta_0 \sqrt{\frac{g}{H}} \sin \left(\frac{\omega}{\sqrt{gH}} (L - x) \right) \frac{\sin \omega t}{\cos \left(\frac{\omega}{\sqrt{gH}} L \right)}; \quad (5.36)$$

$$v(x, y, t) = 0. \quad (5.37)$$

Since the wind stress, bottom friction, and coriolis force terms are ignored, the solution corresponds only to the interaction between the incident wave and the reflected waves from the wall at $x = L$. For the time integration scheme, we adopt the Euler method of second order to discretize equations (5.28) and (5.29) which yields

$$\zeta^{n+1} = \zeta^n - \Delta t H \{ \nabla \cdot \mathbf{V} \}^n + \frac{(\Delta t)^2}{2} H g \{ \nabla^2 \zeta \}^n, \quad (5.38)$$

$$\mathbf{V}^{n+1} = \mathbf{V}^n - \Delta t g \{ \nabla \zeta \}^n + \frac{(\Delta t)^2}{2} H g \{ \nabla^2 \cdot \mathbf{V} \}^n. \quad (5.39)$$

In the computation, the excitation wave period is taken to be 12 hours and the wavelength is calculated to be 605 km. To compare the methods with consistency, all results are generated with time step sizes $\Delta t = 30$ seconds and the shape parameter $r = 0.815 d_{\min}$. The root-mean-square (RMS) error of the tidal level (ζ) and water velocity (u) calculated by global MQ and multizone MQ models in relation to the analytical solution are analyzed. The RMS results of three of the interpolation points $N = 87, 99, \text{ and } 111$ which are situated in the central of the basin and the requirement of the computational time (CPU) are summarized in Table 2. The root-mean-square error is calculated by

$$\text{RMS} = \sqrt{\frac{1}{T_n} \sum_{i=1}^{T_n} \left(\zeta_i^{\text{analytical}} - \zeta_i^{\text{computed}} \right)^2}, \quad (5.40)$$

where T_n is the total number of time steps, and is taken as $T_n = 1400$, $\zeta_i^{\text{analytical}}$ is the analytical solution, $\zeta_i^{\text{computed}}$ is the simulated results.

By comparing the RMS errors in Table 2, the error of the computed tidal level and velocities of the global scheme and the multizone scheme appear to be of the same order of magnitude. This indicates that the simulated results of the multizone MQ scheme is as good as the global

Table 2. Root-mean-square error (m).

	Global MQ			Four Zones MQ		
N	87	99	111	87	99	111
Tide level (ζ)	9.251×10^{-3}	1.181×10^{-2}	1.010×10^{-2}	6.486×10^{-3}	1.111×10^{-2}	1.039×10^{-2}
Water current (u)	3.783×10^{-3}	5.623×10^{-3}	1.412×10^{-2}	5.094×10^{-3}	7.887×10^{-3}	1.257×10^{-2}
CPU time for 100 time steps	106 seconds			41 seconds		

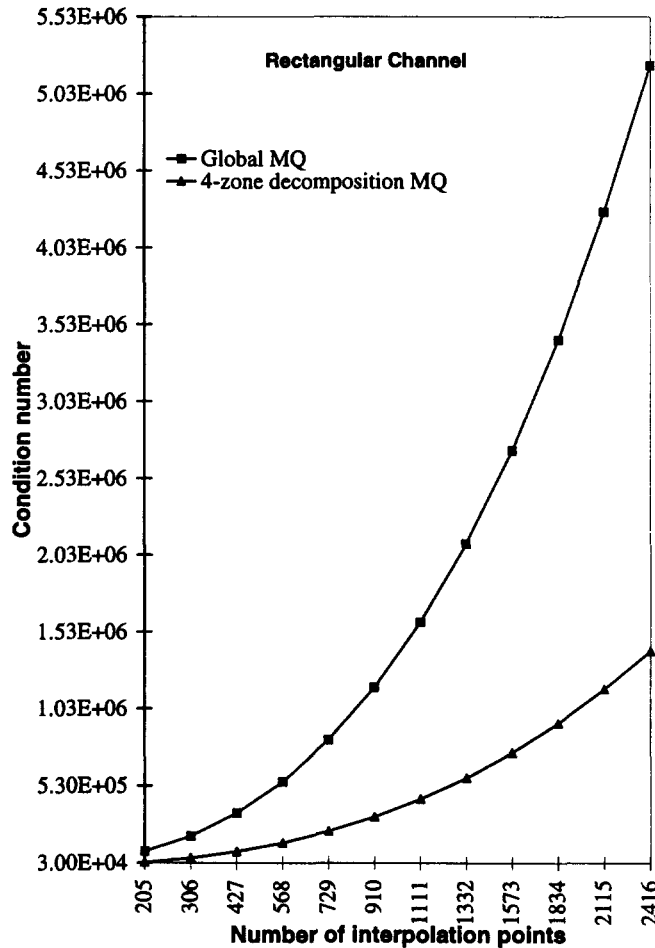


Figure 4. Condition numbers versus interpolation points for the global MQ and multizones MQ model.

MQ scheme. Regarding the computational efficiency, multizone MQ performed more efficiently with a saving of 61% in CPU time comparing to the global MQ scheme.

To further assure the superiority of the multizone decomposition MQ scheme over the global MQ scheme, the condition numbers of the coefficient matrices of the radial basis function for the two schemes with different number of interpolation points were compared. For simplicity, we only illustrate the condition numbers of the proposed decomposition MQ scheme for the rectangular channel model with four zones. The reader should be aware that the value of the condition number can be reduced by dividing the region into further division. For the multizone scheme, the average condition numbers of the four zones were used for comparison. The results are presented in Figure 4. We can see from the figure that the condition number of the coefficient matrix for the global scheme increases rapidly with increase in interpolation points while for the

multizone scheme, the rate of increase of condition number is much less. This indicates that for global scheme, the coefficient matrix will become ill-conditioned with increase in interpolation points but not for the case of the multizone scheme.

CASE 2. A NONLINEAR WATER FLOW MODEL. A hypothetical model is studied in Case 1 where the analytical solution is available to compare with the computed solution. In this case, the application of the multizone MQ scheme is applied to a real-life model. We use Tolo Harbour of Hong Kong as a reference test case for a two-dimensional nonlinear hydrodynamic model. The MQ scheme has been successfully applied to solve a system of water quality equations to this harbour with 260 data points in our previous study [6]. The construction of the multizone MQ scheme is based on the same set of data points. These 260 data points are distributed evenly as indicated in Figure 5.

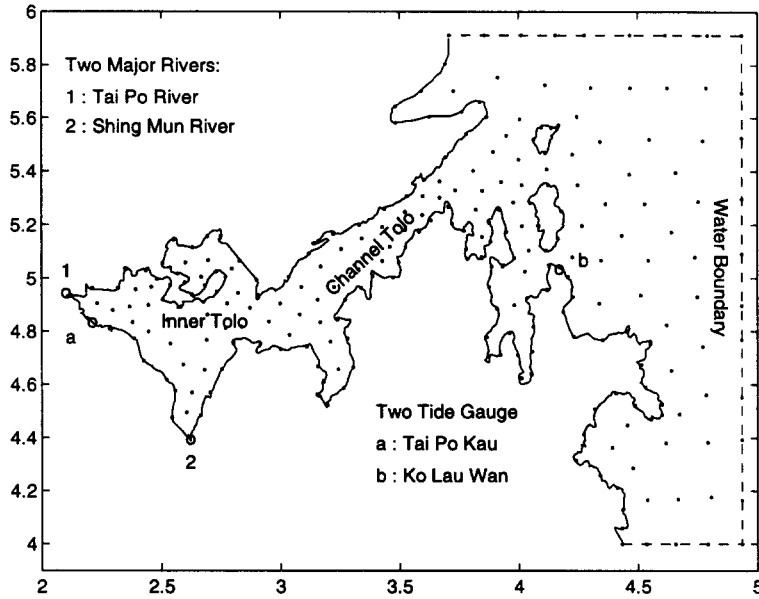


Figure 5. Map of the Tolo Harbour of Hong Kong showing the location of tide gauges, main rivers. The dot (•) distributed on the map represents the interpolation points.

Tolo Harbour is a semi-enclosed embayment with a very irregular coastline that surrounds its land boundary, this typical geographical condition makes it well suited to verify the application of the method. The embayment occupies an area of 50 km² and is 16 km long. The width of the embayment varies from 5 km in the inner basin to just over 1 km at the mouth of the harbour. The tide in Tolo Harbour is a mixed semidiurnal type with a tidal period of 24.5 hours. The overall range of the tidal level is around 0.1 m to 2.7 m. The measurement of the current flows is recorded as an average 10 cm/sec in the channel of the harbour. The water depth of Tolo Harbour is shallow in Inner Tolo Harbour with less than 10 m deep and is deeper in Channel Tolo more than 20 m.

The simulation is done for the period between 1 February 1991 and 30 April 1991. We choose $N = 260$ collocation points in the whole domain Ω of which 23 are on the water boundary; 107 are interior points, and 130 are on the land boundary. The tide and wind stress data are obtained from the Observatory of Hong Kong. Both tide and wind data are the average hourly observed data at the tide gauges. The location of two tide gauges are indicated in Figure 5. To satisfy the water-water boundary condition as defined in equation (2.2), the input surface elevation ζ^n on water-water boundary is estimated using the equation suggested by the Observatory of Hong Kong given as

$$\zeta^n(x_i, y_i, t) = \zeta^*(t + T_{COR,i}) + H_{COR,i} \quad \text{for } i = 1, 2, \dots, 23, \quad (5.41)$$

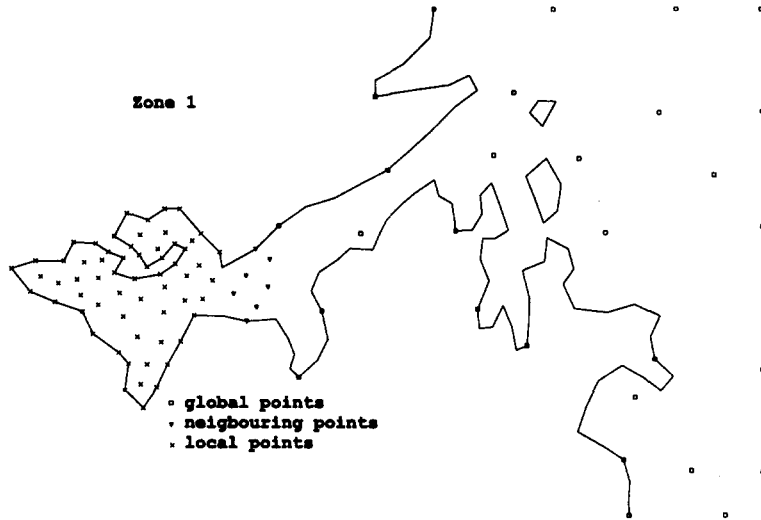


Figure 6. Computational Zone 1 showing the distribution of data points.

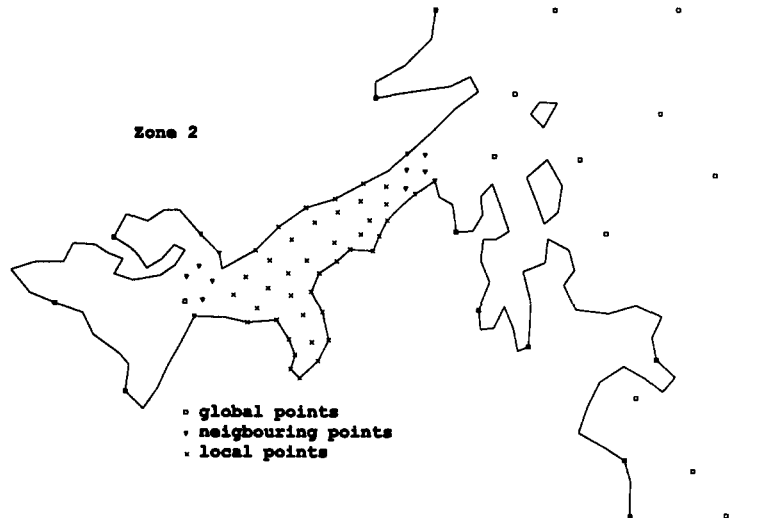


Figure 7. Computational Zone 2 showing the distribution of data points.

where $\zeta^*(t)$ is the actual tide data measured at a tide gauge, T_{COR_i} is the time correction parameter, H_{COR_i} is the tide level correction parameter.

The model is tested using the multizone decomposition scheme with five and seven zones. Each computational zone consists of roughly a same number of collocation points with 80 to 90 points in five-zone model and 60 to 70 points in seven-zone model in the set $(W^k \cup B^k \cup S^k)$. To reduce the spurious oscillation caused by the two islands in the harbour, we specially assigned more points in the zone containing these two islands. Figures 6–10 show the allocation of data points in the model of five zones. In the figures, the notation \times denotes points in W^k , ∇ denotes points in B^k , and \square denotes points in S^k . The performance of the multizone decomposition MQ scheme exhibits reasonable stability and accuracy throughout the three months simulation period. Figure 11 shows the comparison of the computational results between the global MQ and the multizone MQ in 260 collocation points for the period between 23 February 1991 and 27 February 1991.

In order to investigate the effect of density of data points on the performance of the global MQ simulation, we repeat the simulation with several sets of data points ranging from 260 to 200. We removed a number of points at a time from the regions with small height gradient that are not close to the open sea and land boundaries. These removed points should have the least impact

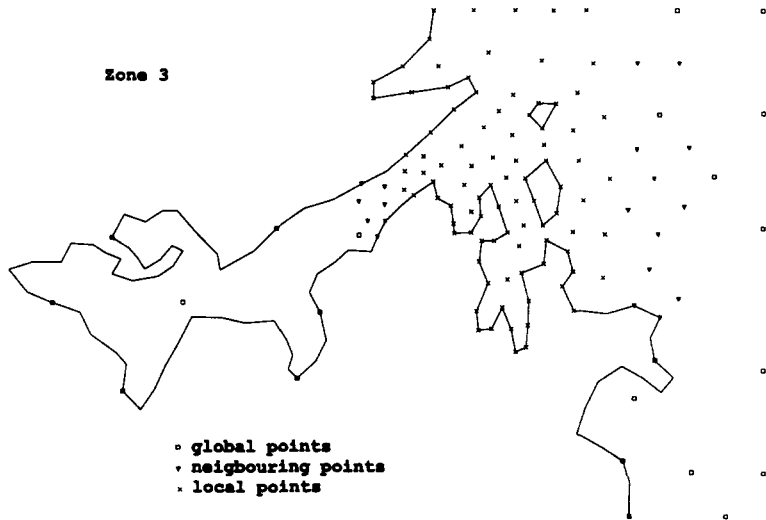


Figure 8. Computational Zone 3 showing the distribution of data points.

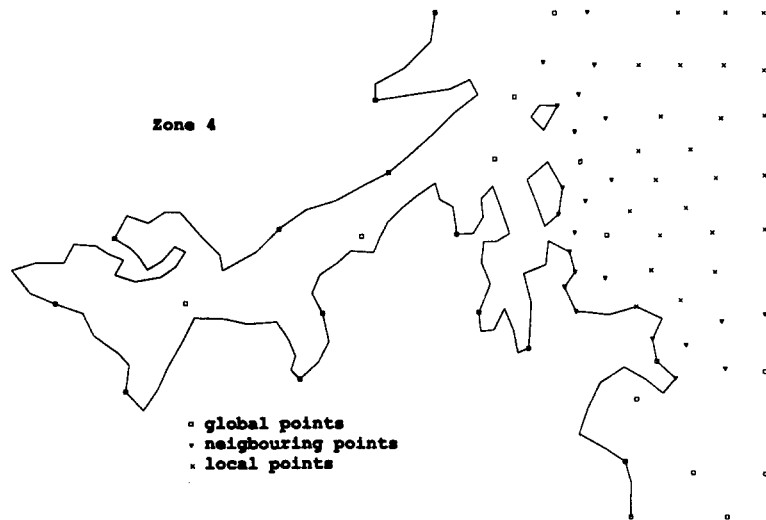


Figure 9. Computational Zone 4 showing the distribution of data points.

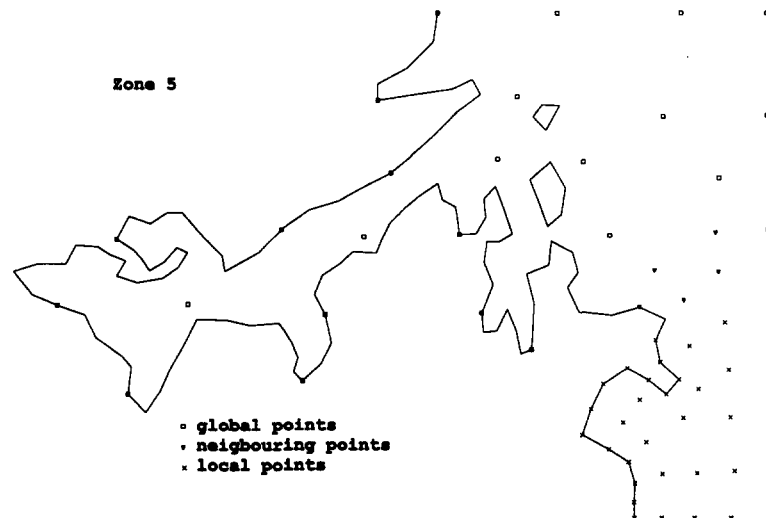


Figure 10. Computational Zone 5 showing the distribution of data points.

on the simulated results, because the rate of change of water flow is considered to be insignificant there.

In view of the numerical experiments when using time step $\Delta t = 30$ seconds and a constant $r = 0.815d_{\min}$, the results indicate that the performance of the global MQ model degrades gradually with smaller number of data points. It becomes significantly unsteady with model of less than 200 data points.

Table 3 compares the observed data at Ko Lau Wan tide gauge with the simulated results of the various models. Both the root-mean-square error and absolute maximum error are presented. The simulation is carried out for a total number of hours $T_n = 2036$ with time step size of 30 seconds.

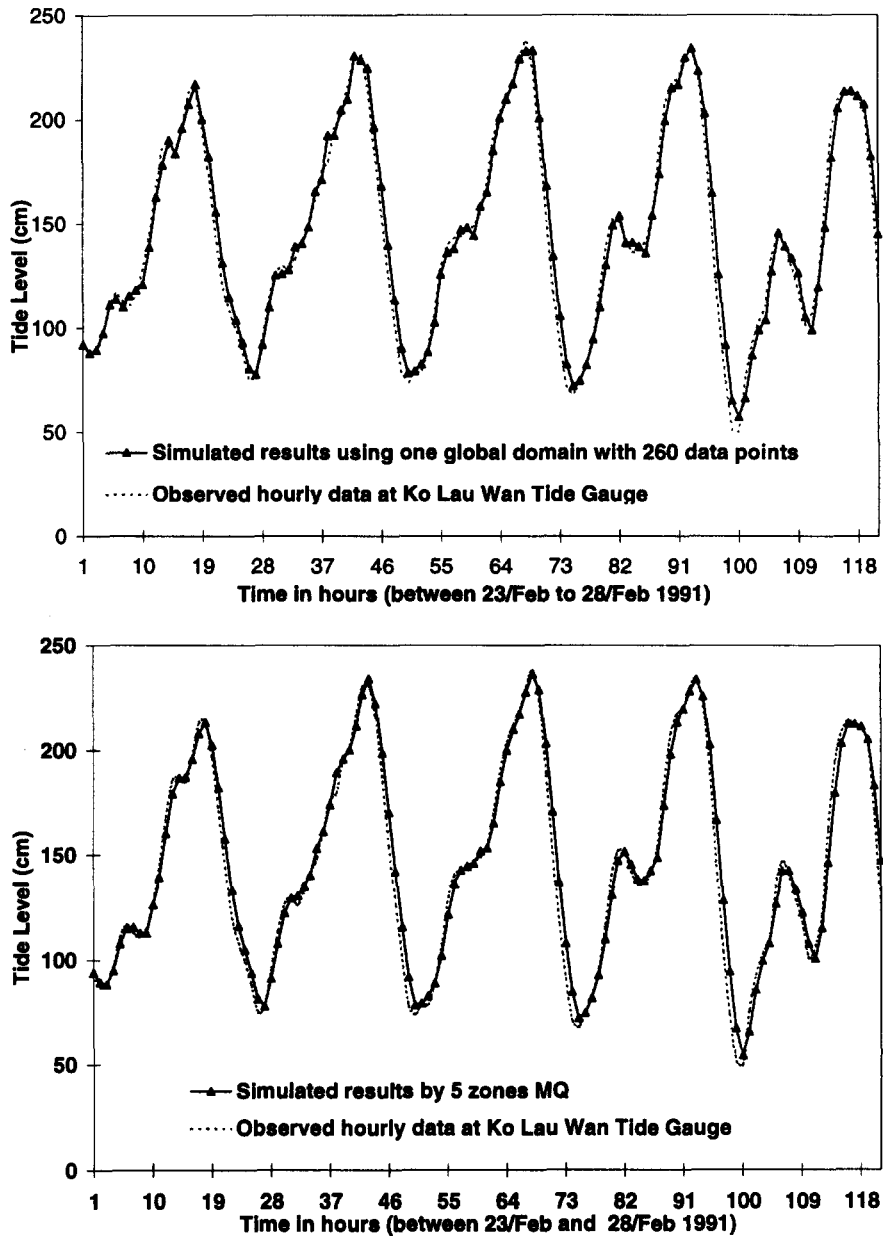


Figure 11. Comparison of the simulated values of the global MQ and the multi-zone MQ in five and seven zones in 260 data points with the observed hourly tide level in Tolo Harbour from 23 February to 28 February 1991.

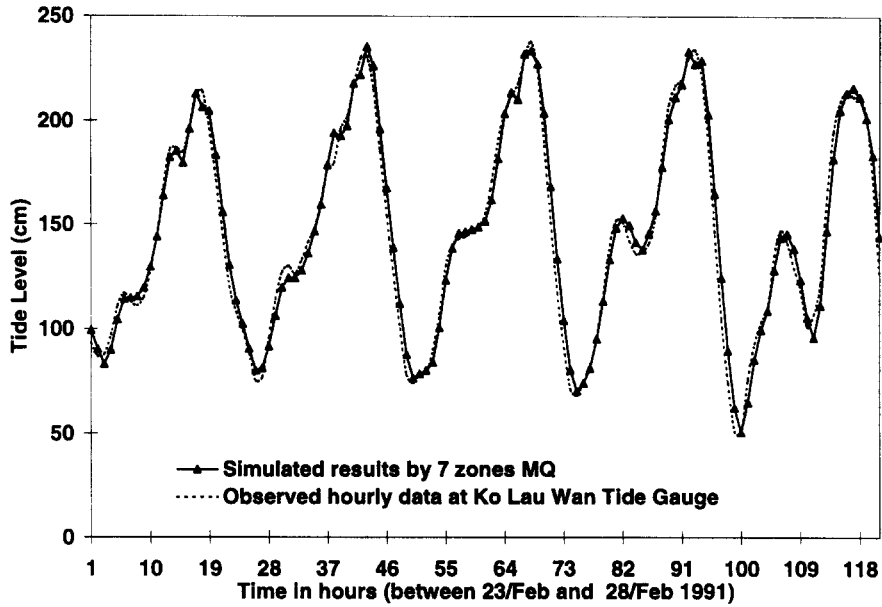


Figure 11. (continued)

Table 3. Analysis of the tidal level for the interpolation point at a tide gauge of the Tolo Harbour, $\Delta t = 30$ seconds, $r = 0.815d_{\min}$.

	Root-Mean-Square Error (m)	Absolute Max. Error (m)	CPU Time For 10^3 Time Steps
260 nodes global MQ	7.615×10^{-2}	2.469×10^{-1}	993 seconds
210 nodes global MQ	1.058×10^{-1}	3.185×10^{-1}	706 seconds
five zones MQ	7.906×10^{-2}	2.467×10^{-1}	575 seconds
seven zones MQ	7.570×10^{-2}	2.392×10^{-1}	481 seconds

The CPU time for 10^3 time steps is also shown in Table 3. By comparing the root-mean-square error, it is observed that the accuracy of the multizone decomposition MQ models are very close to the global MQ with 260 data points. Multizone decomposition can effectively reduce the computational time by 42% in five zones and 51% in seven zones with only an relative computational error of around 4% when compared with the global MQ result in 260 data points. On the other hand, the global MQ with 210 collocation points produced a relatively large RMS error. In spite of the fact that computational time is considerably reduced with fewer collocation points, numerical experiments show a deterioration of computational accuracy.

The eddy and flood velocities of the multizone decomposition MQ in five and seven zones are compared with those results of the global MQ with 260 points in Figures 12–14. These figures show that there are no significant difference in the overall pattern of the current velocities between these three models. It indicates that smoothness in distribution of velocities across zone boundaries can be maintained in the multizone MQ models. Since there is no regular monitoring of the current velocities in the Tolo Harbour, the prediction of the current velocities cannot be verified precisely at a single point. However, previous field measurement of the current flow is recorded at an average of 10 cm/sec in the channel and has a poor flushing rate in the inner harbour, which is consistent with the numerical predictions.

6. CONCLUSION AND DISCUSSION

The application of the multizone decomposition technique to the multiquadric scheme has been described and successfully applied to solve a linear and a nonlinear two-dimensional hydrodynam-

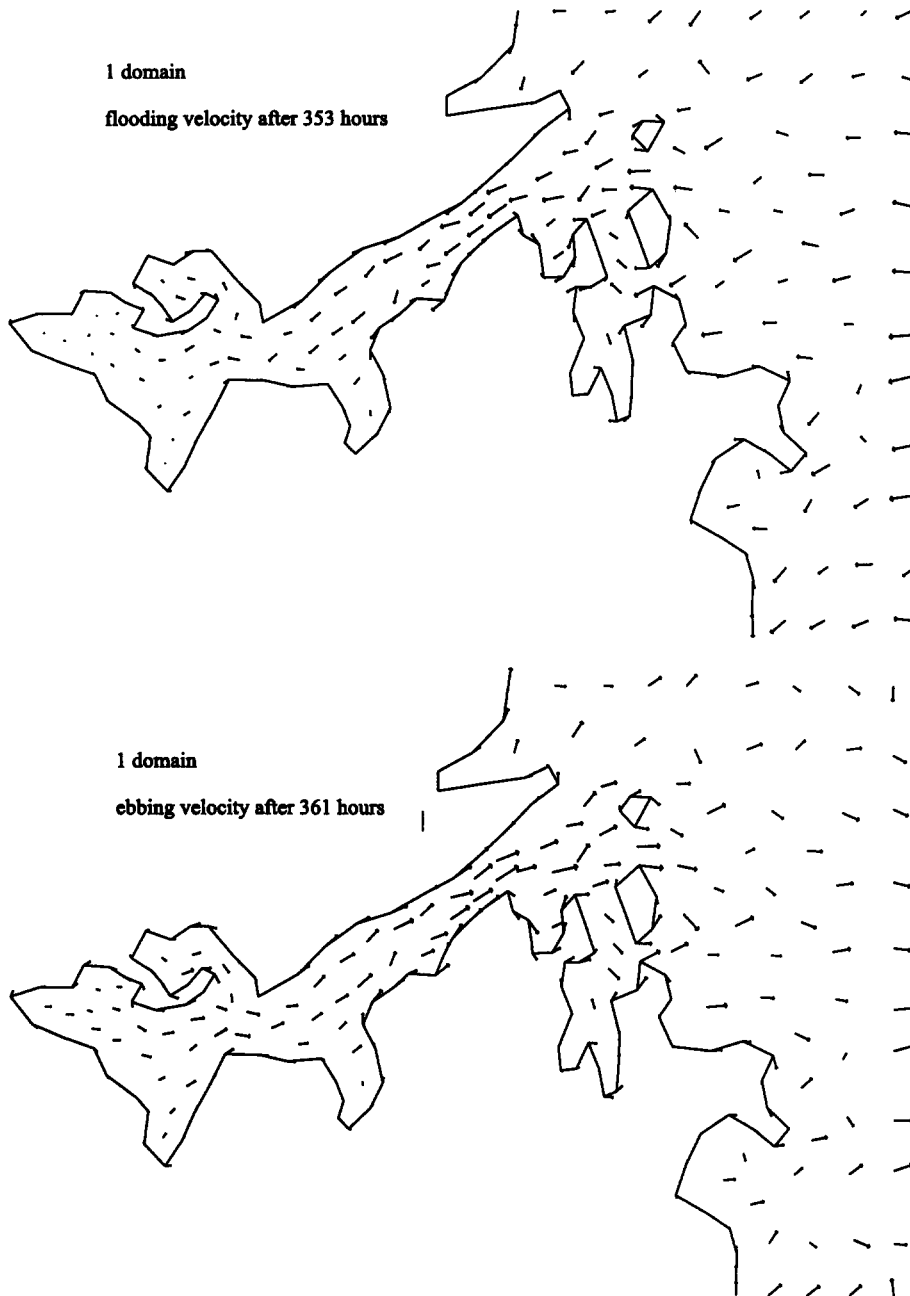


Figure 12. Distribution of the eddy and flood velocities in Tolo Harbour at 353 and 361 hours using global MQ with 260 points.

ics model. In the example of the model in Tolo Harbour, the region under study with 260 data points was divided into five zones and seven zones, respectively. The numerical results and the computing time were compared with those results from the global MQ in a single domain. The multizone MQ model has shown to be an efficient scheme with a saving of more than 40% and 50% of computational time in the five-zone and seven-zone, respectively. Our analysis also shows that the accuracy of the proposed scheme was comparable to that of using a single domain.

Although using radial basis functions to solve partial differential equations provides a simply accurate and truly mesh free algorithm. It is known that when the multiquadric scheme is applied to solve large scale problems with a large number of data points, the resulting collocation matrix is very ill-conditioned and the computation is inefficient. To overcome these problems, the

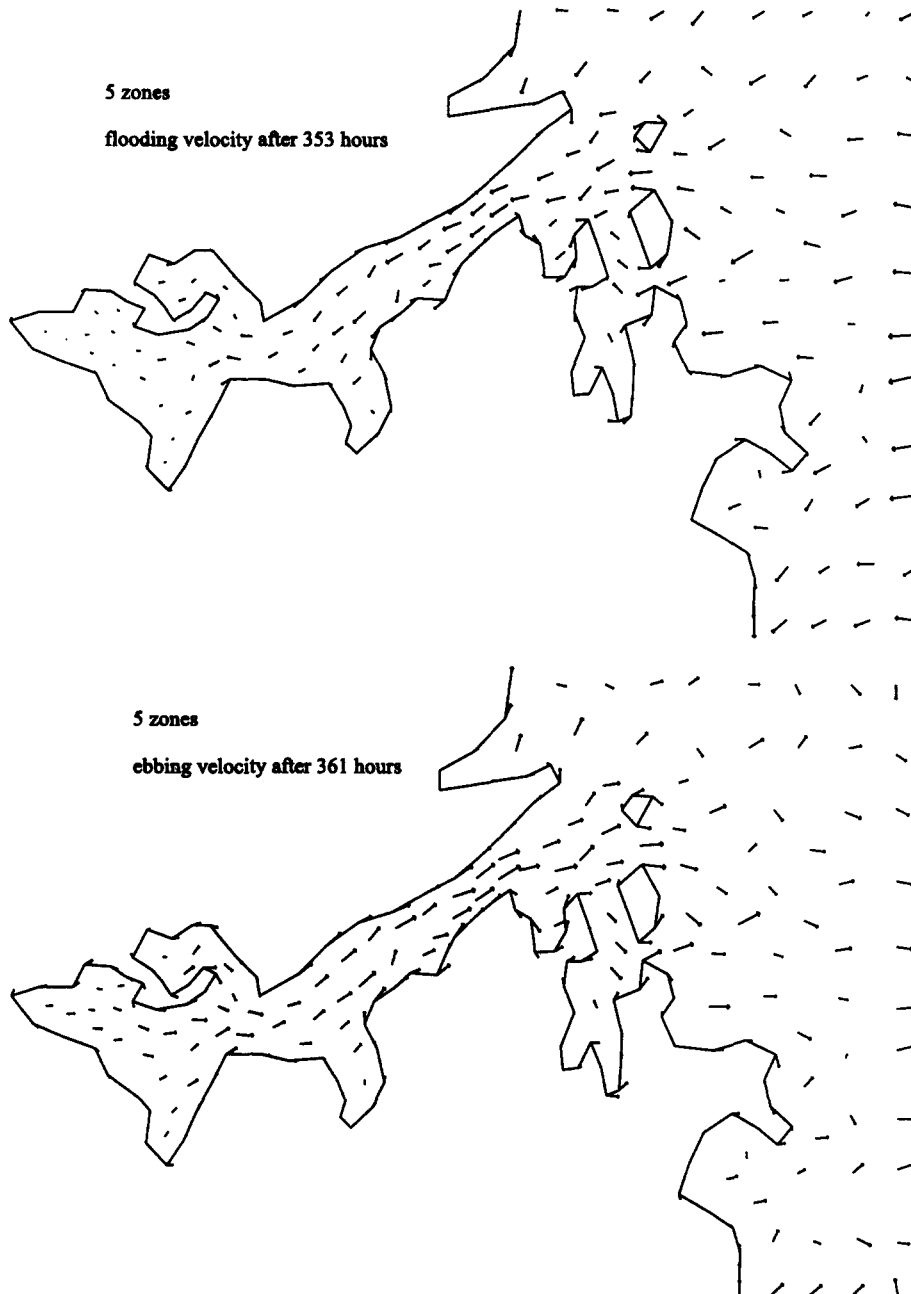


Figure 13. Distribution of the eddy and flood velocities in the Tolo Harbour at 353 and 361 hours using five-zone MQ.

proposed scheme in this paper applied the technique of multizone decomposition to work with the basis functions locally at different zones of resolution. This gives a chance to improve the ill-conditioning problem by the reduction of the size of the full coefficient matrix to be solved. The proposed scheme will make the multiquadric method more feasible for the solving of large-scale or three-dimensional problems. The method also lends itself well to parallel computation with multiple processors, where parallelization across zones are possible. This parallel processing approach is currently under investigation by the authors.

Furthermore, an alternative method using the multilevel approximation approach with compactly supported radial basis functions (RBFs) has been introduced by Floater and Iske [14]. The basic idea of this method is to use a preset compactly supported RBFs to approximate solutions

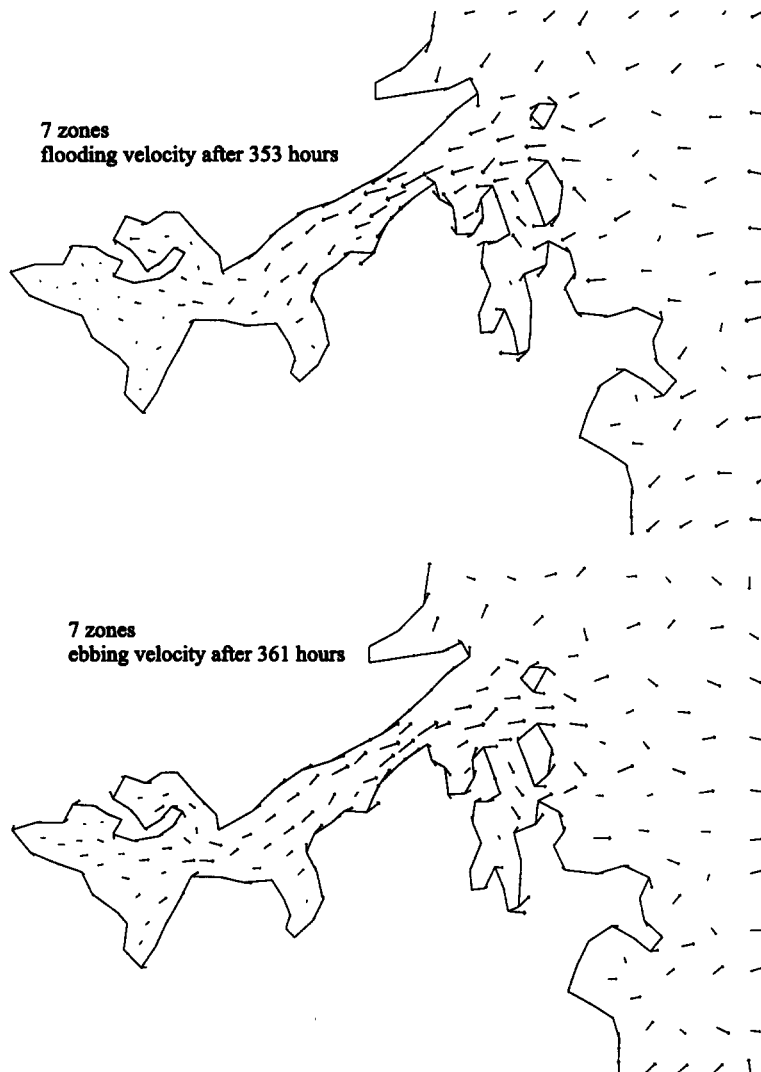


Figure 14. Distribution of the eddy and flood velocities in the Tolo Harbour at 353 and 361 hours using seven-zone MQ.

locally at different levels, the approximate residuals obtained in the finer levels are subsequently added to the coarse level, thus the improvement of the stability and accuracy can be achieved. However, the amount of work involved in computing differentiable residuals at each level is enormous and the procedure would generate additional errors. Fasshauer [15] has recently suggested using a precomputed hierarchy of smooth functions to improve the efficiency of the multilevel approximation with the use of the RBFs. We have made no attempt to give numerical justification and verification to this alternative method as they are beyond the scope of study in this report. The comparison between the multilevel approximation with compactly supported basis functions and the present proposed multizone decomposition scheme will be investigated in the future.

REFERENCES

1. R.L. Hardy, Multiquadric equations of topography and other irregular surfaces, *J. Geophys. Res.* **176**, 1905–1915 (1971).
2. E.J. Kansa, Multiquadric—A scattered data approximation scheme with applications to computational fluid dynamics—I, *Computers Math. Applic.* **19** (8/9), 127–145 (1990).
3. E.J. Kansa, Multiquadric—A scattered data approximation scheme with applications to computational fluid dynamics—II, *Computers Math. Applic.* **19** (8/9), 147–161 (1990).

4. Y.C. Hon, M.W. Lu, W.M. Xue and Y.M. Zhu, Multiquadric method for the numerical solution of a biphasic mixture model, *J. Applied Math & Computation* **88**, 153–175 (1997).
5. Y.C. Hon and X.Z. Mao, A multiquadric interpolation method for solving initial value problem, *J. Scientific Computing* **4** (1), 51–55 (1997).
6. A.S.M. Wong, Y.C. Hon, S.L. Chung and K.C. Ho, A computational model for monitoring water quality and ecological impacts in marine environments, *J. Applied Science & Computations* **12** (1), 75–97 (1997).
7. R.E. Carlson and T.A. Foley, The parameter R^2 in multiquadric interpolations, *Computers Math. Applic.* **21** (9), 29–42 (1991).
8. E.J. Kansa and R.E. Carlson, Improved accuracy of multiquadric interpolation using variable shape parameters, *Computers Math. Applic.* **24** (12), 99–120 (1992).
9. M.A. Golberg, C.S. Chen and S.R. Karur, Improved multiquadric approximation for partial differential equations, *Engineering Analysis with Boundary Elements* **18**, 9–17 (1996).
10. C.A. Micchelli, Interpolation of scattering data: Distance matrices and conditionally positive definite functions, *Constr. Approx.* **2**, 11–12 (1986).
11. M.D.J. Powell, The theory of radial basis function approximation in 1990, In *Advances in Numerical Analysis*, Volume II, pp. 105–210, Clarendon Press, Oxford, (1992).
12. E.J. Kansa, A strictly conservative spatial approximation scheme for the governing engineering and physics equations over irregular regions and homogeneously scattered nodes, *Computers Math. Applic.* **24** (5/6), 169–190 (1992).
13. M.R. Dubal, Domain decomposition and local refinement for multiquadric approximations. I: Second-order equations in one-dimension, *J. Applied Science & Computation* **1** (1), 146–171 (1994).
14. M.S. Floater and A. Iske, Multistep scattered data interpolation using compactly supported radial basis functions, *J. Comput. Applied Math.* **73**, 65–78 (1996).
15. G.E. Fasshauer, On smoothing for multilevel approximation with radial basis functions, In *Proceedings of 9th International Conference on Approximation Theory*, Nashville, TN, pp. 1–8, (1998).
16. R.E. Carlson and B.K. Natarajan, Sparse approximation multiquadric interpolations, *Computers Math. Applic.* **27** (6), 99–108 (1994).